Nitriding characteristics of 4H-SiC irradiated with remote nitrogen plasmas

Masaharu Shimabayashi[1]*, Kazuaki Kurihara[2], Yoshimine Horikawa[1], and Koichi Sasaki[1]

[1]*Division of Quantum Science and Engineering, Hokkaido University, Sapporo 060-8628, Japan*
[2]*Corporate Research and Development Center, Toshiba Corporation, Kawasaki 212-8582, Japan*

We examined the atomic concentrations and the weight densities of SiC surfaces irradiated with remote nitrogen plasmas. The unique approach of this work is that we compared the SiC surface irradiated with atomic nitrogen with that irradiated with a mixture of atomic nitrogen and molecular nitrogen in the metastable $A^3\Sigma_u^+$ state. As a result, it was found that molecular nitrogen in the $A^3\Sigma_u^+$ state has a higher efficiency than atomic nitrogen in the nitriding of SiC surfaces. The weight density measurements have revealed the removal of Si and C from the SiC surface by the irradiation of remote nitrogen plasma. These results suggest that the formation of volatile molecules is less significant when the SiC surface is irradiated with molecular nitrogen in the metastable $A^3\Sigma_u^+$ state.

1. Introduction

Various technologies for energy saving are of great importance to solve environmental problems and to realize a sustainable society. The development of power transistors, which are used as switching devices in electric power systems, is a key issue.[1–3)] Silicon carbide (SiC) is the material that will be used in irradiated with in the next-generation power devices because of its high insulation voltage and robustness against high temperature.[4–6)] In addition, a metal-oxide-semiconductor field-effect transistor (MOSFET) based on SiC has the advantages of low on-resistance and high switching speed.[7–9)] However, the on-resistance of SiC-based MOSFET under development is much higher than the theoretical expectation, which results in a large voltage drop, significant heat generation, and a low efficiency of electronic power systems.

The high on-resistance of SiC-based MOSFET is caused by the low channel mobility in the channel region under the gate insulation film.[10–12)] The small channel mobility is considered to be due to defects around the interface between the channel region and the gate insulation film. Therefore, a method is required to passivate the surface of SiC before depositing

*E-mail: shima@athena.qe.eng.hokudai.ac.jp

the gate insulation film.[13] A solution to this issue, which has been proposed on the basis of a first-principle calculation,[14] is the nitriding of the SiC surface. Although thermal nitriding using NO, N_2O, and NH_3 has been carried out to date, the performance of the passivation is insufficient.[15]

Another method for the nitriding of the SiC surface is irradiation with a nitrogen plasma. Nitrogen-containing plasmas are widely used in surface nitriding of various materials such as metals,[16,17] insulators, and semiconductors.[18,19] However, the surface nitriding using nitrogen-containing plasmas has a problem in that there is a lack of understanding of the effective reactive species. Nitrogen plasmas have three types of reactive species: atomic nitrogen (N), molecular nitrogen at the metastable $A^3\Sigma_u^+$ state [$N_2(A^3\Sigma_u^+)$], and ionized molecular nitrogen (N_2^+).[20] In a previous work, we compared the efficiencies of the three reactive species used for the nitriding of silicon surface.[21] As a result, we have shown that $N_2(A^3\Sigma_u^+)$ and N_2^+ have higher efficiencies than N.

In this work, we examined the nitriding characteristics of the SiC surface using a remote nitrogen plasma source. We chose the remote plasma source since we expected damage of formation on the SiC surface after irradiation with ionic species.[22] The unique approach of this work is that we compared the SiC surface irradiated with N with that irradiated with a mixture of N and $N_2(A^3\Sigma_u^+)$. The fluxes of N and $N_2(A^3\Sigma_u^+)$ were measured by vacuum ultraviolet absorption spectroscopy (VUVAS)[23–25] and cavity ringdown absorption spectroscopy (CRDS),[25–27] respectively. We examined the nitrogen concentration and the weight density of SiC surfaces irradiated with the remote nitrogen plasmas.

2. Experimental procedure

The remote plasma source used in this experiment is schematically shown in Fig. 1. The main chamber was made of stainless steel and had a diameter of 30 cm and a height of 13 cm. A slender quartz tube with a diameter of 8 mm was attached to the top of the vacuum chamber. The chamber was evacuated using a turbo molecular pump below 1×10^{-7} Torr before feeding nitrogen gas. Pure nitrogen gas was fed from the top of the quartz tube at a flow rate of 288 ccm, and the nitrogen pressure in the chamber was adjusted to 0.5 Torr by reducing the pumping speed using a gate valve. A microwave resonator was attached from outside of the quartz tube. The resonator was connected to a microwave power supply at 2.45 GHz via a coaxial cable, a waveguide convertor, a rectangular waveguide, a three-stab tuner, a power monitor, and an isolator. The microwave power was 100 W. A nitrogen plasma was thus produced in a limited region around the microwave resonator by surface-wave (surfertron)

discharge. The microwave resonator was movable in the axial direction of the quartz tube, so that the distance between the active discharge plasma and the SiC sample was changed between 7 and 12 cm.

A load lock chamber was attached to the side of the main chamber. A 4H-SiC sample with a size of 14×14 mm^2 was installed in the load lock chamber and was transferred to a manipulator in the main chamber. The sample was pretreated with 5% hydrogen fluoride solution for 10 min. The manipulator was used for adjusting the position of the sample with respect to the quartz tube. The temperature of the sample was not controlled.

We investigated the nitriding characteristics of the carbon-side surface (C-face) of 4H-SiC in this experiment, since it is reported that MOSFETs constructed on the C-face have a higher channel mobility than those constructed on the Si-face.[28,29)]

The sample irradiated with the remote nitrogen plasma was transferred back to the load lock chamber and was exposed to the atmosphere. The atomic composition on the sample surface was analyzed by X-ray photoelectron spectroscopy (XPS) and high-resolution Rutherford back scattering (HRRBS). The weight density of the sample surface was analyzed by X-ray reflectometry (XRR).

The N atom density in the gas phase was measured by VUVAS, and we adopted CRDS for measuring $N_2(A^3\Sigma_u^+)$ density. Since the details of the two diagnostics were shown previously,[30)] we describe them briefly here. In the N density measurement by VUVAS, the spatial afterglow of the remote nitrogen plasma was placed between an electron cyclotron resonance nitrogen plasma (the light source) and a VUV monochromator. Two MgF_2 windows were used for separating the remote nitrogen plasma, light source plasma, and VUV monochromator. The intensity of a line emission at 120.0 nm (the $^4S^o - ^4P$ transition) yielded from the light source plasma was determined using a secondary-electron multiplier tube via the VUV monochromator. N density was deduced from the absorption of the line emission. In the measurement of $N_2(A^3\Sigma_u^+)$ density by CRDS, the spatial afterglow of the remote nitrogen plasma was sandwiched by two concave mirrors with high reflectivities, which from an optical cavity. We injected a cw diode laser beam into the cavity via an acousto-optic modulator (AOM), and determined the intensity of the laser beam transmitted through the cavity. The laser wavelength was tuned at approximately 771.100 nm, which corresponded to the $B^3\Pi_g(v' = 2) - A^3\Sigma_u^+(v'' = 0)$ absorption band of N_2. The rapid truncation of the laser beam, by triggering AOM at the moment when the cavity length was resonant with the laser wavelength, resulted in an exponential decay of the transmitted laser intensity. $N_2(A^3\Sigma_u^+)$ density was deduced from the decay time constant (the ringdown time). The temperature of $N_2(A^3\Sigma_u^+)$

was evaluated from the Doppler broadening of the absorption line.

3. Results

3.1 Fluxes of N and $N_2(A^3\Sigma_u^+)$

In a previous paper, we reported the N density, the $N_2(A^3\Sigma_u^+)$ density, and the temperature of $N_2(A^3\Sigma_u^+)$ at the sample position in the present experiment.[30] On the basis of these experimental data, we plotted the fluxes of N and $N_2(A^3\Sigma_u^+)$ as a function of the distance between the microwave resonator and the sample, as shown in Fig. 2. The temperature of N is assumed to be the same as that of $N_2(A^3\Sigma_u^+)$. The flux of N_2^+ is also plotted in Fig. 2, which was evaluated from the ion saturation current density of a Langmuir probe at a bias voltage of -50 V with respect to the ground potential. As shown in the figure, the flux of N_2^+ was much lower than the fluxes of N and $N_2(A^3\Sigma_u^+)$. The fluxes of $N_2(A^3\Sigma_u^+)$ and N_2^+ decreased almost exponentially with the distance between the microwave resonator and the measurement position, whereas we observed a slight decrease in the N flux. From Fig. 2, it can be said that the sample was irradiated by atomic nitrogen with a flux of 7.9×10^{15} $cm^{-2}s^{-1}$ when the distance between the sample and the microwave resonator was 12 cm, whereas the mixture of N with a flux of 1.3×10^{16} $cm^{-2}s^{-1}$ and $N_2(A^3\Sigma_u^+)$ with a flux of 2.5×10^{15} $cm^{-2}s^{-1}$ irradiated the sample when the distance between the sample and the microwave resonator was 7 cm.

3.2 Analyses of SiC surface

Figure 3 shows the nitrogen concentrations, which were evaluated by XPS analyses, on the C-face of 4H-SiC samples irradiated with the remote nitrogen plasmas. The measurement position corresponded to the center of the quartz tube. The duration of the irradiation was 1 minute. The nitrogen concentrations shown in Fig. 3 are the averages of several samples, and the error bars show the maximum and minimum values. The atomic concentrations obtained at two distances of 7 and 12 cm between the sample and the microwave resonator are compared. As shown in the figure, the irradiation with the remote nitrogen plasma at a distance of 7 cm from the microwave resonator resulted in a higher nitrogen concentration.

Figure 4 shows the two-dimensional distributions of the nitrogen concentrations on C-face 4H-SiC. The origin of the space coordinate in Fig. 4 corresponds to the center of the quartz tube. These maps were reconstructed from the nitrogen concentrations measured at 35 positions. The spot sizes of the X-ray used in the XPS analyses was 0.5 mm in Figs. 4(a) and 4(b), and the measurement step was 2 mm. The higher nitrogen concentration was observed in the entire region of the sample surface when the distance between the sample and

the microwave resonator was 7 cm. In addition, it is noted from Fig. 4(a) that the distribution of the nitrogen concentration was sharper when the distance between the sample and the microwave resonator was 7 cm. The nitrogen concentration on the sample prepared at a distance of 12 cm from the microwave resonator was lower and had a broader distribution as shown in Fig. 4(b).

We extended the irradiation duration for 3 min and examined the nitrogen concentration at the center of C-face 4H-SiC. The nitrogen concentration on the sample prepared at a distance of 7 cm from the microwave resonator was 6.9 ± 0.6%, whereas the sample prepared at a distance of 12 cm had a nitrogen concentration of 2.4 ± 0.1%. Compared with the nitrogen concentrations shown in Fig. 3, which were obtained after the irradiation for 1 miniute, the nitrogen concentration is saturated against the dose.

Figure 5 shows the XPS spectra of the N 1s peak, which were observed on the C-face of 4H-SiC samples irradiated with the remote nitrogen plasmas. The duration of the plasma irradiation was 3 min. The distances between the microwave resonator and the sample were 7 and 12 cm in Figs. 5(a) and 5(b), respectively. The spectra were deconvoluted by assuming two peaks corresponding to N-Si and N-O_x bondings.[31] As shown in the figure, the N-Si component was more dominant when the distance between the microwave resonator and the sample was 7 cm.

Figure 6 shows the depth profiles of the atomic concentrations, which were obtained by HRRBS analyses, at the centers of the C-face substrate irradiated with the remote nitrogen plasmas. The duration of the irradiation was 3 min. The depth profiles of the channeling coefficients, which show the degree of deviation from the perfect crystal, are also plotted in Fig. 6. As shown in the figure, the higher nitrogen concentration obtained by the irradiation of the remote nitrogen plasma at a distance of 7 cm was confirmed by the HRRBS analysis. In addition, it is noted from Fig. 6(a) that the SiC surface irradiated at a distance of 7 cm had a deeper nitride layer. The channeling coefficients in the nitride layers were 100%, indicating that the crystalline structure of SiC was broken completely in the nitride layer. Another point shown in Fig. 6 is the lower concentrations of Si and C on the nitride surface. The concentration of C was especially low, and the top surface of the sample was changed into SiO_2 by the irradiation of the remote nitrogen plasma. The impurity oxygen was considered to be mixed into the sample when it was exposed to the atomosphere.

Table I shows the weight densities of the samples in the regions at depths of $d \leq 1.1$, $1.1 \leq d \leq 1.7$, and $d \geq 1.7$ nm from the top surfaces, together with the weight density of virgin SiC.

This result was obtained by the XRR analysis. As shown in the table, the SiC surfaces irradiated with the remote nitrogen plasmas had lower weight densities than virgin SiC. The lower weight densities with low carbon concentrations indicate the removal of C from the SiC surface by the irradiation with the remote nitrogen plasma.

Table I also suggests the removal of Si since the weight density of SiO_2 is 2.2 g/cm^3. In addition, it should be emphasized here that the weight density at the top surface of SiC prepared at a distance of 7 cm was higher than that prepared at a distance of 12 cm.

4. Discussion

As shown in Fig. 2, the dependence of the flux on the distance between the microwave resonator and the sample position was significantly different in N and $N_2(A^3\Sigma_u^+)$. This difference is due to the difference in the kinetics and the surface loss probabilities of these reactive species. As shown in a previous paper, atomic nitrogen has a small surface loss probability on material surfaces.[32] In addition, the interaction between atomic nitrogen and the surface of the quartz tube is moderated by the laminar gas flow under the present experimental condition. Because of the small surface loss probability and the laminar gas flow, the lifetime of atomic nitrogen in the quartz tube is long, resulting in the slight decrease in the N flux with the distance from the microwave resonator. On the other hand, the lifetime of $N_2(A^3\Sigma_u^+)$ is expected to be short because of the high surface loss probability. It is impossible to transport $N_2(A^3\Sigma_u^+)$ from the active plasma region to the sample. According to Guerra et al., $N_2(A^3\Sigma_u^+)$ is produced in the spatial afterglow of a nitrogen plasma due to the mechanism called V-V pumping-up.[33] The location where the V-V pumping-up mechanism is active is determined by gas pressure and gas flow rate, and the relationship between the $N_2(A^3\Sigma_u^+)$ flux and the distance shown in Fig. 2 is determined by the position with active V-V pumping-up. In this experiment, we utilized the above difference in the kinetics and the surface loss probabilities of N and $N_2(A^3\Sigma_u^+)$ for controlling the composition of reactive species supplied to the sample.

As shown in Fig. 2, the flux of N_2^+ was, at least, two orders of magnitude lower than the fluxes of N and $N_2(A^3\Sigma_u^+)$. Considering the fact that the contributions of $N_2(A^3\Sigma_u^+)$ and N_2^+ to the nitriding of silicon are similar,[21] the contribution of N_2^+ is expected to be negligible in the present experiment because of the negligible flux. As described in Sect. 3.1, the N flux at a distance of 7 cm was approximately 1.6 times higher than that at a distance of 12 cm.

However, we cannot attribute the higher nitrogen concentration at 7 cm shown in Fig. 3 to the higher N flux, since the nitrogen concentration was saturated against the dose of atomic nitrogen. The saturation of the nitrogen concentration against the dose is confirmed by com-

paring the absolute number of the dose with the number of atomic nitrogen in the sample. The number of atomic nitrogen in the unit area of the sample is on the order of $10^{14} - 10^{15}$ cm^{-2}, as shown in Table I and Fig. 6, whereas the dose of atomic nitrogen is on the order of 10^{18} cm^{-2} when the duration of the irradiation is 3 min. Therefore, the difference in the N flux by a factor of 1.6 cannot cause the higher nitrogen concentration at 7 cm, and it is attributed to the difference in the composition of active species. That is, the experimental results suggest the dominant contribution of $N_2(A^3\Sigma_u^+)$ to the nitriding of SiC. Since the $N_2(A^3\Sigma_u^+)$ flux was lower than the N flux by a factor of 3-5, it is suggested that $N_2(A^3\Sigma_u^+)$ has a higher efficiency than atomic nitrogen for the nitriding of the SiC surface. The importance of $N_2(A^3\Sigma_u^+)$ has also been observed in the nitriding of silicon.[21)]

Another possibility is the contribution of atomic nitrogen at the metastable ^2D state ($N(^2D)$). From the measurements shown in the previous paper, the $N(^2D)$ density at a distance of 7 cm was roughly one-half of the $N_2(A^3\Sigma_u^+)$ density.[30)] In the previous experiment for the nitriding of silicon using inductively coupled plasmas, we did not detect the contribution of $N(^2D)$ even though its density was similar to the density of atomic nitrogen at the ground state.[21)] Under the present experimental condition, the density (the flux) of $N(^2D)$ was much lower than that of ground-state atomic nitrogen. In addition, since the production kinetics of $N(^2D)$ is different from that of $N_2(A^3\Sigma_u^+)$, the decrease in the $N(^2D)$ density with the distance from the microwave resonator was gentler than that in the $N_2(A^3\Sigma_u^+)$ density.[30)] Therefore, we believe that $N_2(A^3\Sigma_u^+)$ has a more significant contribution than $N(^2D)$ to the nitriding of SiC.

The experimental results shown in Fig. 4 support the dominant contribution of $N_2(A^3\Sigma_u^+)$ to the nitriding of SiC. Figure 7 shows the radial distribution of the optical emission intensity at the second positive system of molecular nitrogen, which was observed below the exit of the quartz tube when removing the sample. The optical emission intensity was obtained by integrating the band spectrum of the second positive system along the wavelength. The radial distribution was obtained by applying the Abel inversion to the line-integrated optical emission intensities. As shown in Fig. 7, the optical emission intensity of the second positive system showed a peaky distribution. The optical emission of the second positive system in the spatial afterglow is due to the production of $N_2(C^3\Pi_u)$ via $N_2(A^3\Sigma_u^+) + N_2(A^3\Sigma_u^+) \rightarrow N_2(C^3\Pi_u) + N_2(X^1\Sigma_g^+)$, since the electron density and electron temperature in the sample region were 7.7×10^8 cm^{-3} and 0.4 eV, respectively. The electron density and electron temperature were measured using a Langmuir double probe. When $N_2(C^3\Pi_u)$ is produced by the collision of two $N_2(A^3\Sigma_u^+)$ molecules, the radial distribution of

the optical emission intensity roughly represents the square of $N_2(A^3\Sigma_u^+)$ density. Therefore, the significant distribution of the nitrogen concentration on the sample surface prepared at a distance of 7 cm [Fig. 4(a)] is due to the peaky distribution of the $N_2(A^3\Sigma_u^+)$ density. Since the radial distribution of the N density is expected to be flat because of the long lifetime, the less significant distribution of the nitrogen concentration on the sample surface prepared at a distance of 12 cm [Fig. 4(b)] suggests the dominant contribution of atomic nitrogen to the nitriding when the $N_2(A^3\Sigma_u^+)$ flux is negligibly low.

The depth profiles of atomic concentrations shown in Fig. 6 indicate the low nitrogen concentrations on the top surfaces. Since the transport mechanism of nitrogen in the sample is diffusion, it is speculated that the depth profiles of the nitrogen concentration shown in Fig. 6 are formed when the samples are exposed to the atmosphere. That is, nitrogen around the top surface is desorbed and is replaced by oxygen.

The experimental results shown in Fig. 6 suggests that $N_2(A^3\Sigma_u^+)$ works efficiently for forming the nitride layer in the deeper region below the oxide layer. The further diffusion of oxygen is stopped by the nitride layer. The formation of the robust nitride layer with the help of $N_2(A^3\Sigma_u^+)$ is confirmed by the dominant N-Si bonding in the XPS spectrum shown in Fig. 5(a). In addition, another qualitative difference in the nitride layer, which is formed with the help of $N_2(A^3\Sigma_u^+)$ is seen in Table I.

Figure 6 shows the removal of carbon (and silicon) from the top surface of SiC by the irradiation of the remote nitrogen plasma. The possible volatile molecules are HCN and C_2N_2. On the other hand, the weight densities shown in Table I indicate that the removal is less significant when the distance between the sample and the microwave resonator is 7 cm, even though the nitriding is more efficient. This suggests the possibility of a low-damage nitriding process using $N_2(A^3\Sigma_u^+)$.

5. Conclusions

In this work, we compared carbon-side surfaces of SiC irradiated with atomic nitrogen and the mixture of atomic nitrogen and molecular nitrogen at the metastable $A^3\Sigma_u^+$ state. The experimental results indicate the higher efficiency of $N_2(A^3\Sigma_u^+)$ than N for the surface nitriding of SiC. In addition, the SiC surface irradiated with $N_2(A^3\Sigma_u^+)$ had a deeper nitride layer and a higher weight density. The present experimental results suggest the possibility of an efficient, low-damage nitriding process using $N_2(A^3\Sigma_u^+)$.

References

1) T. Kimoto, Jpn. J. Appl. Phys. **54**, 040103 (2015).
2) P. G. Neudeck, J. Electron. Mater. **24**, 283 (1995).
3) S. Ryu, C. Capell, E. Van Brunt, C. Jonas, M. O'Loughlin, J. Clayton, K. Lam, V. Pala, B. Hull, Y. Lemma, D. Lichtenwalner, Q. J. Zhang, J. Richmond, P. Butler, D. Grider, J. Casady, S. Allen, J. Palmour, M. Hinojosa, C. W. Tipton, and C. Scozzie, Semicond. Sci. Technol. **30**, 084001 (2015).
4) K. Ito, S. Tsukimoto, and M. Murakami, Sci. Technol. Adv. Mater. **7**, 496 (2006).
5) A. Frazzetto, F. Giannazzo, R. L. Nigro, V. Raineri, and F. Roccaforte, J. Phys. D **44**, 255302 (2011).
6) I. Pesic, D. Navarro, M. Fujinaga, Y. Furui, and M. Miura-Mattausch, Jpn. J. Appl. Phys. **54**, 04DP11 (2015).
7) M. Bhatnagar and B. J. Baliga, IEEE Trans. Electron Devices **40**, 645 (1995).
8) J. Biela, M. Schweizer, S. Waffler, and J. W. Kolar, IEEE Trans. Electron Devices **58**, 2872 (2011).
9) A. Itoh,T. Kimoto, and H. Matsunami, IEEE Electron Device Lett. **16**, 139 (1996).
10) S. L. Rumyantsev, M. S. Shur, M. E. Levinshtein, P. A. Ivanov, J. W. Palmour, A. K. Agarwal, B. A. Hull, and Sei-Hyung Ryu, Semicond. Sci. Technol. **24**, 075011 (2009).
11) H. Yano, T. Hirao, T. Kimoto, H. Matsunami, K. Asano, and Y. Sugawara, IEEE Electron Device Lett. **20**, 611 (1999).
12) G. Y. Chung, C. C. Tin, J. R. Williams, K. McDonald, R. K. Chanana, R. A. Weller, S. T. Pantelides, L. C. Feldman, O. W. Holland, M. K. Das, and J. W. Palmour, IEEE Electron Device Lett. **22**, 176 (2001).
13) H. O. Olafsson, G. Gudjonsson, P.-A. Nilsson, E. O. Sveinbjornsson, H. Zirath, T. Rodle, and R. Jos, Electron. Lett. **40**, 508 (2004).
14) T. Shimizu and T. Shinohe, U.S. Patent 0,199,846A1 (2012)
15) G. Chung, C. C. Tin, J. R. Williams, K. McDonald, M. D. Ventra, R. K. Chanana, S. T. Pantelides, L. C. Feldman, and R. A. Weller, App. Phys. Lett **77**, 3601 (2000).
16) I. Jauberteau, J. L. Jauberteau, M. Cahoreau, and J. Aubreton, J. Phys. D **38**, 3654 (2005).
17) S. Kim, J. Lee, N. Saito, and O. Takai, J. Phys.: Conf. Ser. **417**, 012023 (2013).
18) Y. Fukuda, K. Kato, H. Toyota, T. Ono, Y. Nagasato, and T. Ueno, Jpn. J. Appl. Phys. **45**, 7351 (2006).

19) K. Seo, S. Kim, D. B. Janes, M. W. Jung, K. An, and S. Ju, Nanotechnology. **23**, 435201 (2012).
20) T. Hayashi, K. Ishikawa, M. Sekine, M. Hori, A. Kono, and K. Suu, Jpn. J. Appl. Phys. **51**, 026505 (2012).
21) Y. Horikawa, K. Kurihara, and K. Sasaki, Appl. Phys. Express **4**, 086201 (2011).
22) D. Y. Lee and H. K. Baik, Jpn. J. Appl. Phys. **45**, L376 (2006).
23) K. Sasaki, Y. Kawai, and K. Kadota, Appl. Phys. Lett. **70**, 1375 (1997).
24) K. Sasaki, Y. Kawai, and K. Kadota, Rev. Sci. Instrum. **70**, 76 (1999).
25) Y. Horikawa, K. Kurihara, and K. Sasaki, Jpn. J. Appl. Phys. **49**, 026101 (2010).
26) K. W. Busch and M. A. Busch, Cavity-Ringdown Spectroscopy: An Ultratrace-Absorption Measurement Technique, ed. K. W. Busch and M. A. Busch (Oxford University Press, New York, 1999) [in English].
27) R. Engeln, K. G. Y. Letourneur, M. G. H. Boogaarts, M. C. M. van de Sanden, and D. C. Schram, Chem. Phys. Lett. **310**, 405 (1999).
28) K. Fukuda, M. Kato, K. Kojima, and J. Senzaki, Appl. Phys. Lett. **84**, 2088 (2004).
29) T. Kimoto, Y. Kanzaki, M. Noborio, H. Kawano, and H. Matsunami, Jpn. J. Appl. Phys. **44**, 1213 (2005).
30) Y. Horikawa, T. Hayashi, and K. Sasaki, J. Phys.: Conf. Ser. **441**, 012009 (2013).
31) J. Eng Jr., I. A. Hubner, J. Barriocanal, R. L. Opila, and D. J. Doren, J. Appl. Phys. **95**, 1963 (2004).
32) Y. Horikawa, T. Hayashi, and K. Sasaki, Jpn. J. Appl. Phys. **51**, 126301 (2012).
33) V. Guerra, P. A. Sa, and J. Loureiro, Eur. Phys. J.: Appl. Phys. **28**, 125 (2004).

Table I. Weight densities (g/cm^3) of the SiC surfaces irradiated with remote nitrogen plasmas at distances of 7 and 12 cm from the microwave resonator. The weight density of the virgin 4H SiC is also shown.

	$d \leq 1.1$ nm	$1.1 \leq d \leq 1.7$ nm	$d \geq 1.7$ nm
Irradiated SiC (7 cm)	2.0	2.2	3.21
Irradiated SiC (12 cm)	1.8	3.21	3.21
Virgin SiC		3.21	

Figure captions

Fig. 1 Schematic diagram of the main chamber. The microwave resonator was movable in the axial direction of the quartz tube.

Fig. 2 Fluxes of reactive nitrogen species as a function of the distance from the microwave resonator.

Fig. 3 Average of the nitrogen concentrations on the carbon-side surfaces of several SiC samples irradiated with the remote nitrogen plasmas at z=7 and 12 cm. The error bars are the maximum and minimum values.

Fig. 4 Distributions of the concentrations of atomic nitrogen on the SiC surfaces irradiated with remote nitrogen plasmas at distances of (a) 7 and (b) 12 cm.

Fig. 5 XPS spectra of the N 1s peak observed on 4H-SiC surfaces irradiated with remote nitrogen plasmas at distances of (a) 7 and (b) 12 cm from the samples.

Fig. 6 Depth profiles of the atomic concentrations on the carbon-side surfaces of SiC irradiated with the remote nitrogen plasmas at distances of (a) 7 and (b) 12 cm from the samples.

Fig. 7 Radial distribution of the optical emission intensities obtained by applying Abel inversion to the line-integrated optical emission intensities.

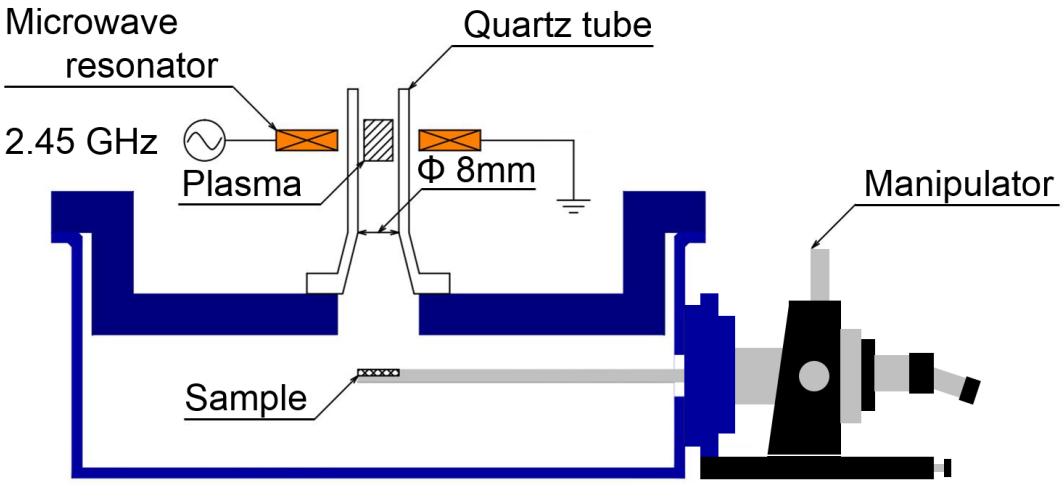

Fig. 1. Schematic diagram of the main chamber. The microwave resonator was movable in the axial direction of the quartz tube.

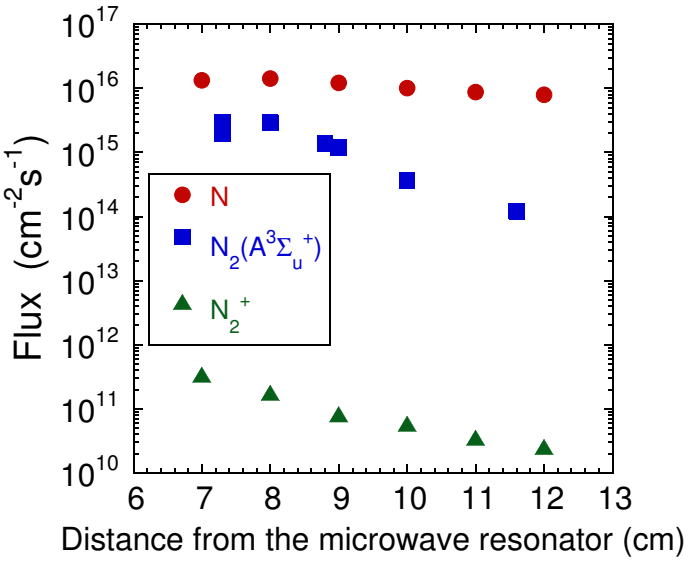

Fig. 2. Fluxes of reactive nitrogen species as a function of the distance from the microwave resonator.

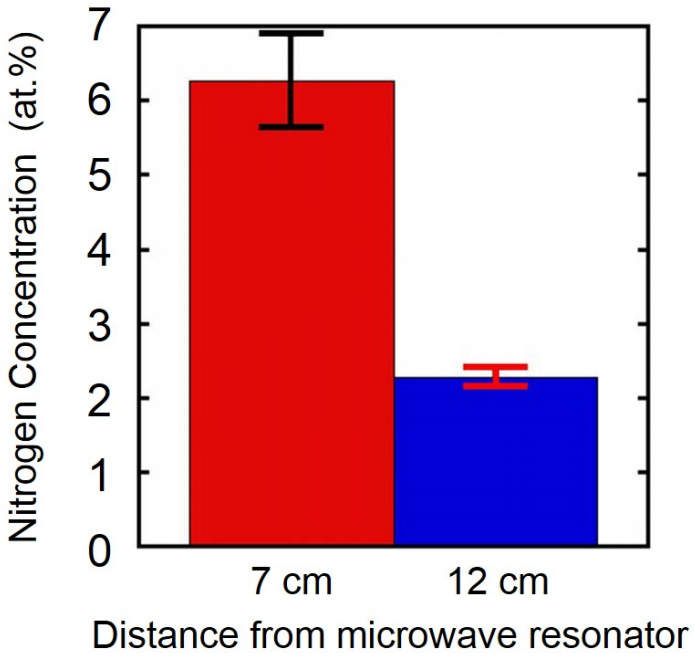

Fig. 3. Average of the nitrogen concentrations on the carbon-side surfaces of several SiC samples irradiated with the remote nitrogen plasmas at z=7 and 12 cm. The error bars are the maximum and minimum values.

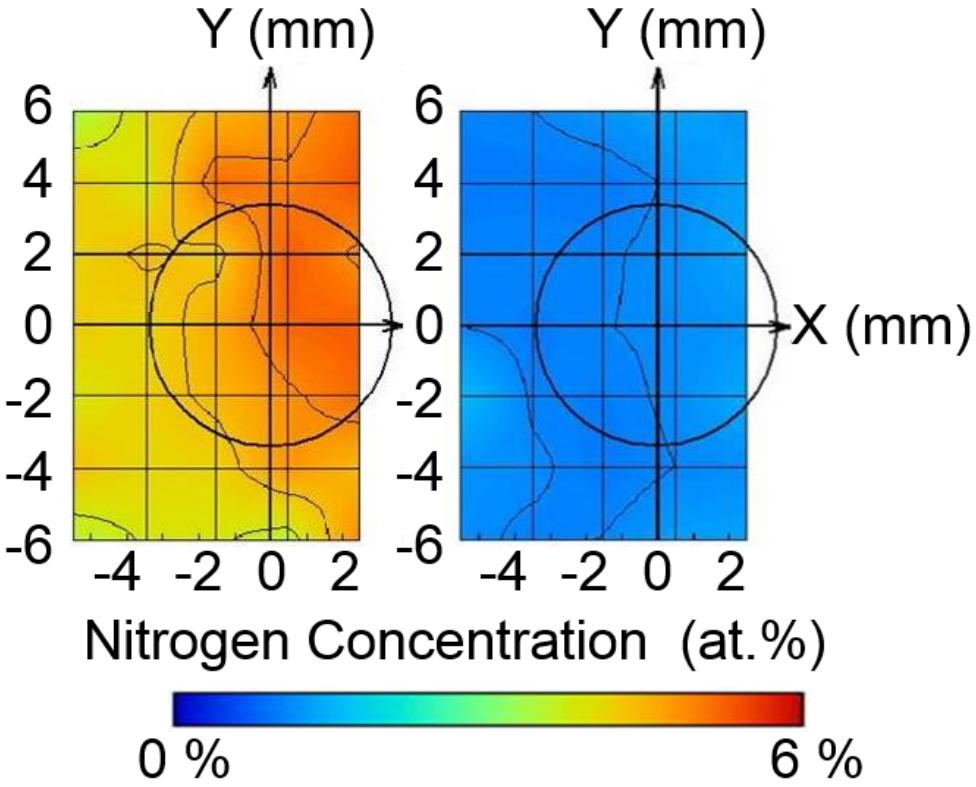

Fig. 4. Distributions of the concentrations of atomic nitrogen on the SiC surfaces irradiated with remote nitrogen plasmas at distances of (a) 7 and (b) 12 cm.

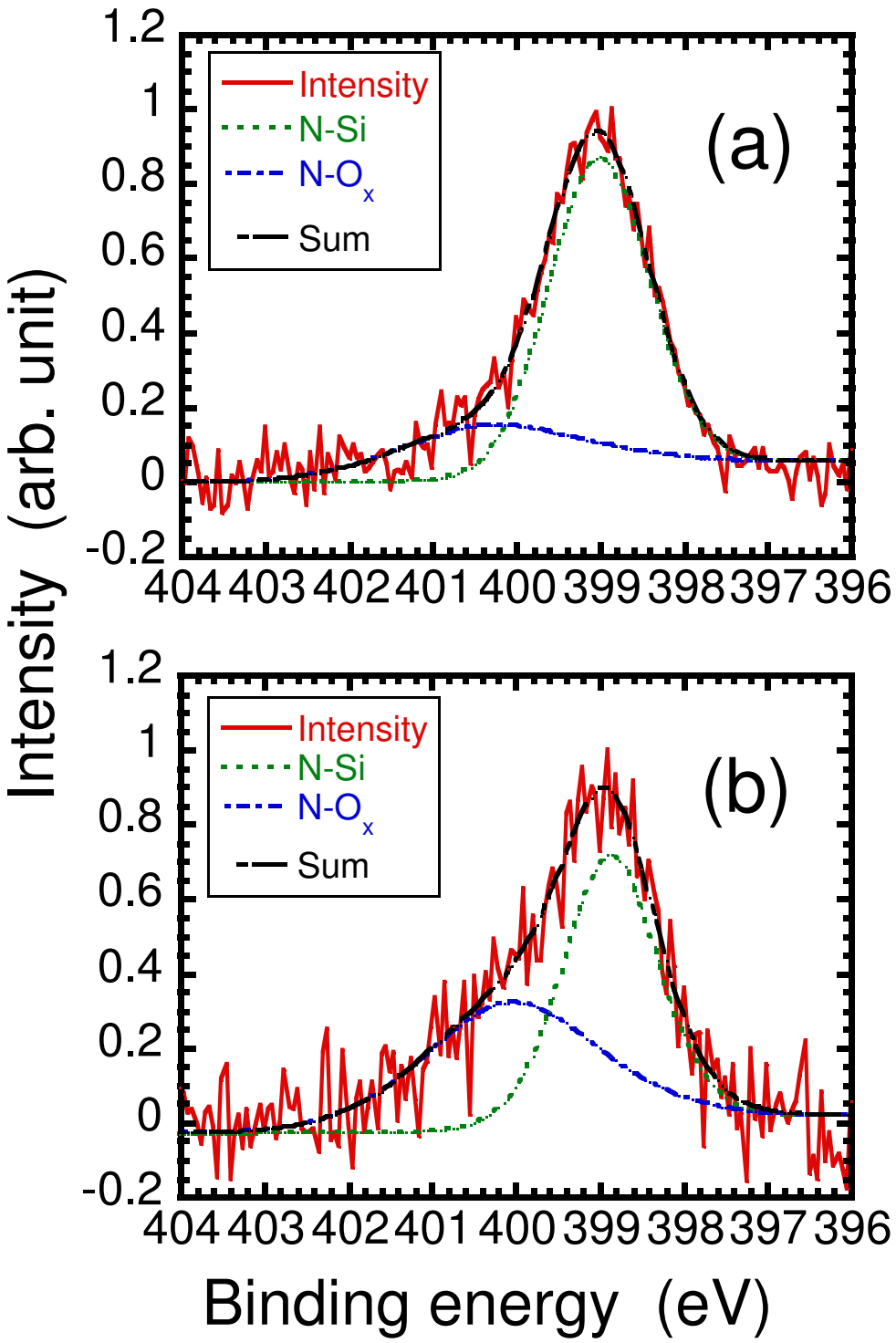

Fig. 5. XPS spectra of the N 1s peak observed on 4H-SiC surfaces irradiated with remote nitrogen plasmas at distances of (a) 7 and (b) 12 cm from the samples.

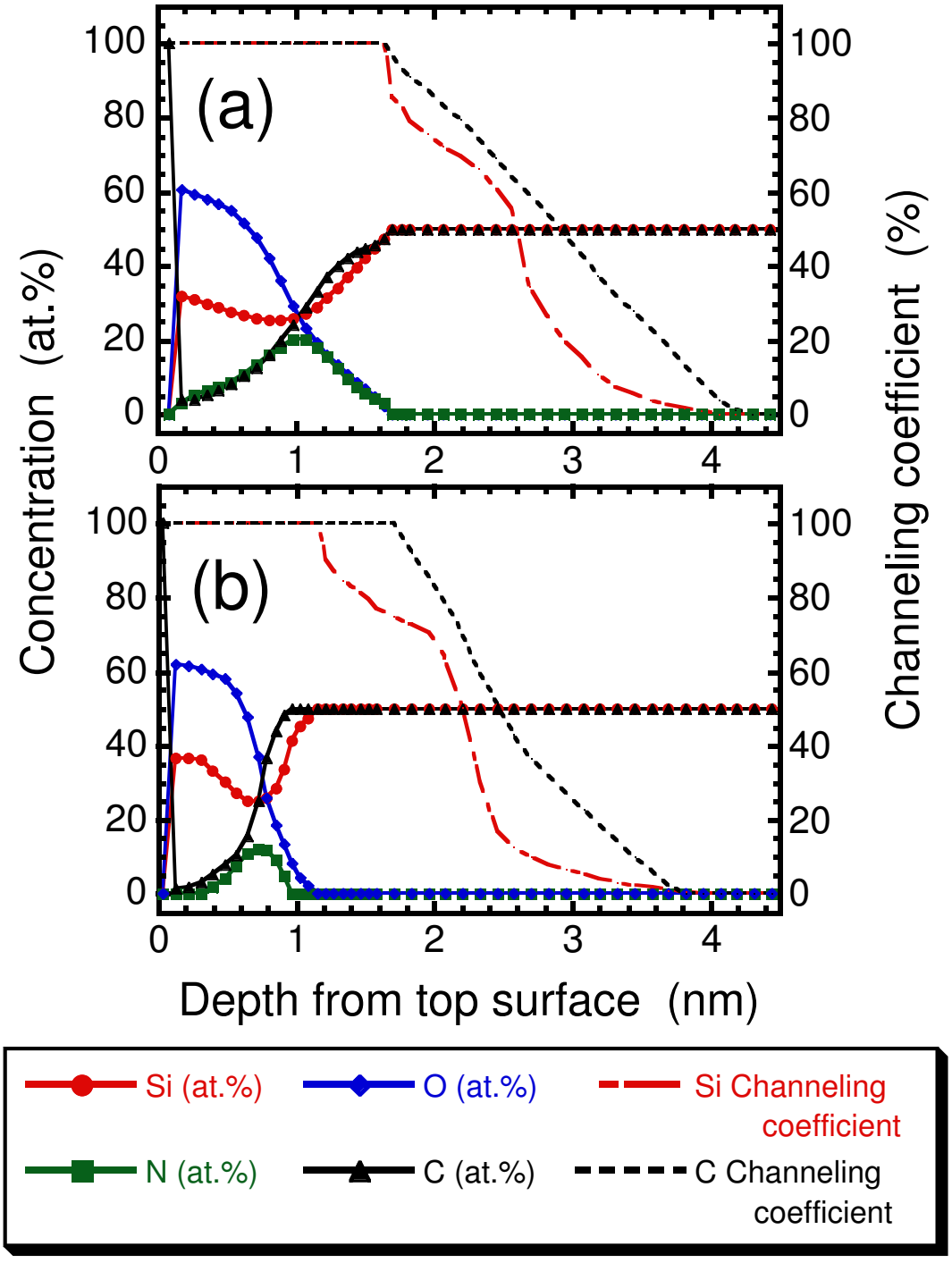

Fig. 6. Depth profiles of the atomic concentrations on the carbon-side surfaces of SiC irradiated with the remote nitrogen plasmas at distances of (a) 7 and (b) 12 cm from the samples.

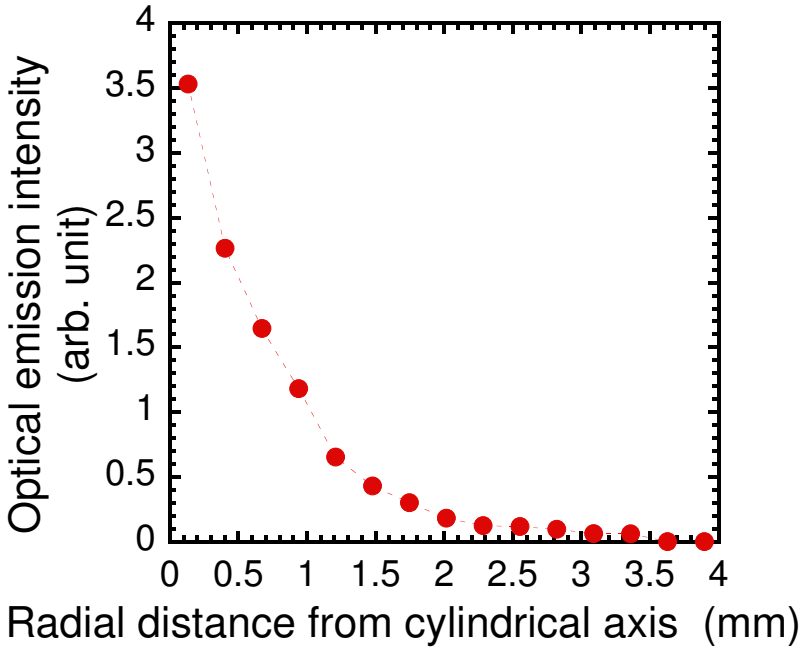

Fig. 7. Radial distribution of the optical emission intensities obtained by applying Abel inversion to the line-integrated optical emission intensities.